Received: 11 September 2020 | Revised: 1 December 2020 | Accepted: 7 December 2020

DOI: 10.1096/fj.202002073R

RESEARCH ARTICLE

THE FASEB JOURNAL

Functional genomics of GPR126 in airway smooth muscle and bronchial epithelial cells

Robert J. Hall | **Jonathan O'Loughlin** | **Charlotte K. Billington** | **Dhruma Thakker** | **Ian P. Hall** | **Ian Sayers**

Division of Respiratory Medicine, National Institute for Health Research, Nottingham Biomedical Research Centre, Biodiscovery Institute, University of Nottingham, Nottingham, UK

Correspondence
Robert Hall, Division of Respiratory Medicine, National Institute for Health Research, Nottingham Biomedical Research Centre, Biodiscovery Institute, University of Nottingham, Nottingham, NG7 2RD, UK.
Email: robert.hall@nottingham.ac.uk

Funding information
Hermes Fellowship University of Nottingham, Grant/Award Number: 2016-2017; British Lung Foundation (BLF), Grant/Award Number: Grant PPRG15-5; RCUK | Medical Research Council (MRC), Grant/Award Number: G1000861; NIHR Senior Investigator award; The Centre of Membrane Proteins and Receptors (COMPARE)

Abstract

GPR126 is an adhesion G protein-coupled receptor which lies on chromosome 6q24. Genetic variants in this region are reproducibly associated with lung function and COPD in genome wide association studies (GWAS). The aims of this study were to define the role of GPR126 in the human lung and in pulmonary disease and identify possible casual variants. Online tools (GTEx and LDlink) identified SNPs which may have effects on GPR126 function/ expression, including missense variant Ser123Gly and an intronic variant that shows eQTL effects on GPR126 expression. GPR126 signaling via cAMP-mediated pathways was identified in human structural airway cells when activated with the tethered agonist, stachel. RNA-seq was used to identify downstream genes/ pathways affected by stachel-mediated GPR126 activation in human airway smooth muscle cells. We identified ~350 differentially expressed genes at 4 and 24 hours post stimulation with ~20% overlap. We identified that genes regulated by GPR126 activation include IL33, CTGF, and SERPINE1, which already have known roles in lung biology. Pathways altered by GPR126 included those involved in cell cycle progression and cell proliferation. Here, we suggest a role for GPR126 in airway remodeling.

KEYWORDS

COPD, cell biology, genomics

1 | INTRODUCTION

Chronic obstructive pulmonary disease (COPD) is a major worldwide cause of morbidity and mortality.[1,2] Treatments can alleviate symptoms yet there is an unmet need for therapeutic interventions that can halt or reverse disease progression. Risk factors for disease development are environmental, including cigarette smoke, and there is also a

Abbreviations: 7TM, 7 transmembrane spanning region; aGPCR, adhesion G Protein-coupled receptor; COPD, chronic obstructive pulmonary disease; CUB, complement C1r/C1s, Uegf, Bmp1; ECD, extracellular domain; ECM, extracellular matrix; eQTL, expression quantitative trait loci; FDR, false discovery rate; FEV1, forced expired volume in 1 second; FVC, forced vital capacity; GAIN, GPCR autoproteolysis-inducing; GPCR, G protein-coupled receptor; GPS, GPCR proteolysis site; GSEA, gene set enrichment analysis; GWAS, genome wide association study; HASM, human airway smooth muscle; HBEC, human bronchial epithelial cell; LD, linkage disequilibrium; PTX, Pentraxin; RNA-seq, RNA-sequencing; SNP, single nucleotide polymorphism.

Ian P. Hall and Ian Sayers contributed equally.

genetic component with recent heritability estimates ranging from 50% to 66%.[3] However, the mechanisms underlying genetic effects are mostly unclear.

Lung function measurements are essential parameters used in the diagnosis of COPD and are, therefore, ideal quantitative traits to use in studies aiming to identify the genetic risk factors for COPD. The most commonly used are forced expired volume in 1 second (FEV_1), forced vital capacity (FVC), and FEV_1/FVC ratio. Using lung function phenotypes for genetic studies allows for additional subjects and, therefore, increased power to detect causal variants with the assumption that the genetics of lung function and COPD share some commonality. The most recent and largest genome wide association study (GWAS) for lung function identified 279 loci showing association with FEV_1, FVC, or FEV_1/FVC.[4] Moreover, GWAS in COPD subjects have identified that there is significant overlap between signals associated with COPD risk and signals associated with lung function measurements.[5] There is now a need to translate GWAS signals to biological understanding by studying the underlying functional effects of the genetic variants in respiratory health and disease.

The 6q24 locus is one that has reproducibly been associated with lung function measurements[5-7] with the most recent GWAS identifying two signals from this locus. First, rs17280293 (A > G) (signal 1) is a missense variant (Ser123Gly) within the coding region of GPR126 which is associated with reduced FEV_1/FVC (risk allele A, allele frequency = 97.3%, beta = −0.1803, and P = 2.34E-131).[4] This signal is also associated with an increase in FVC (P = 8.58E-22).[4]

The second signal (signal 2) comes from an intronic SNP within the GPR126 coding region (rs7753012 (T/G), risk allele T for reduced lung function (FEV_1/FVC), allele frequency = 69.5%, beta = −0.0712, and P = 4.71E-165).[4] This second signal also showed association for reduced FEV_1 (P = 7.09E-23).

Moreover, missense variant Ser123Gly (signal 1) is also associated with diffusing capacity of the lung (D_{LCO}/V_A) (risk allele A, beta = −0.07, and P value = 1.51E–10) even after adjustment for FEV_1/FVC.[8] This study also noted that GPR126 expression was decreased in lung tissue obtained from more severe COPD patients compared with never smokers and in patients with lowered D_{LCO}/V_A compared to normal D_{LCO}/V_A controls.[8]

GPR126 belongs to the adhesion GPCRs (aGPCRs) subfamily of GPCRs. This family has 33 members, defined by the presence of their large N-terminal regions, which can be as large as 6000 amino acids long, in addition to the canonical 7 transmembrane spanning regions (7TM).[9,10] These extracellular regions contain several conserved domains that are important for adhesion interactions. All aGPCRs contain the GPCR autoproteolysis-inducing (GAIN) domain which contains the GPCR proteolysis site (GPS) motif.[11,12] During biosynthesis, aGPCRs are autoproteolysed at this site which results in a cleaved receptor that nonetheless remains associated at the cell surface.[13,14] While the extracellular domain (ECD) is still associated with the 7TM it exerts an inhibitory effect on receptor signaling and it is hypothesized that interaction with a potential ligand or mechanical stimuli would result in removal or rearrangement of the ECD thereby removing the inhibitory effect.[15,16] This reorganisation releases a short peptide sequence which lies C-terminal to the GPS cleavage site (termed stachel). This stachel peptide acts as a tethered agonist and can activate receptor signaling.[17] These receptors can signal via traditional GPCR pathways via G proteins and[18] to date Gα12/13, Gαo, Gαs, Gαi, and Gαq have all been shown to be involved in aGPCR signaling pathways.[15]

GPR126 is one of the more well-studied aGPCRs with known roles in peripheral nerve development, angiogenesis, and inner ear formation via canonical GPCR signaling through G_{as}- and G_{ai}-mediated regulation of intracellular cAMP.[19-25] Complete knockout of GPR126 in mice leads to embryonic lethality due to cardiovascular failure.[26] However, incomplete knockout where the ECD is still present leads to mice which have limb defects, highlighting an independent signaling role for the ECD once dissociated from the 7TM.[23,26,27] A number of potential ligands have been identified for GPR126 including laminin-211 and collagen type IV, which are predicted to involve binding to the complement C1r/C1s, Uegf, Bmp1 (CUB), and pentraxin (PTX) domains in the ECD.[23,28] Ser123Gly (signal 1) lies within the CUB domain and, therefore, could have potential effects on ligand binding. Moreover, recent studies have identified additional mechanisms which modulate GPR126 activity, including the importance of a calcium-binding domain in the ECD, mutations in which lead to defects in myelination and ear development in vivo.[29] Furthermore, alternative splicing of exon 6 (present in 2/4 known isoforms) modulates GPR126 signaling activity.[29] Isoforms lacking exon 6 maintain a closed conformation and show decreased signaling activity compared to those with exon 6, which inhibits the closed conformation.[29]

Polymorphisms in GPR126 have been associated with scoliosis in humans.[18,30-33] One such variant, rs41289839, has been shown to decrease the expression of exon 6, which would be expected to dampen GPR126 signaling activity.[18,29]

Despite advances in understanding of GPR126 function, the role of GPR126 in the human lung is currently unknown and, therefore, the mechanisms by which genetic variants at the *GPR126* locus are associated with lung function are not understood. However, it is known that GPR126 is differentially expressed throughout human lung development, suggesting that it may be important for normal lung development.[34]

We hypothesized that *GPR126* is the causal gene underlying the genetic associations at this locus and that either alteration in protein structure or regulation of the levels of the mRNA/protein underlie this effect. In this study, we aimed to identify potential causal variants within *GPR126* and identify potential mechanisms by which altered GPR126 expression/function may affect airway biology.

2 | MATERIALS AND METHODS

2.1 | RNA isolation

RNA isolation was carried out using the GenElute™ Mammalian Total RNA Miniprep Kit as per the manufacturer's instruction (Sigma).

2.2 | cDNA synthesis

cDNA synthesis was performed using the Superscript First Strand Synthesis System for RT-PCT kit (Invitrogen).

2.3 | Primary bronchial epithelial cell culture

Human Bronchial Epithelial Cells (HBECs) were purchased from Lonza (Wokingham, UK) (Supplementary Table 1). HBECs were maintained in PneumaCult-Ex Basal Medium (490 ml PneumaCult-Ex Basal Medium plus 10 ml PneumaCult-Ex 50X Supplement and 500 µl 200X hydrocortisone stock solution) with the addition of 5 ml of antibiotic, antimycotic solution containing penicillin, streptomycin, and fungizone (PSF).[35]

2.4 | Human airway smooth muscle cell culture

Human lung tissue was obtained from the Nottingham Health Science Biobank or the Papworth Hospital Tissue Bank from patients undergoing lung resection surgery. Human airway smooth muscle (HASM) cells were obtained from lung tissue using the explant model outlined below. Details of these tissue donors can be found in the supplement (Supplementary Table 2). Written consent was obtained from all patients and the study was conducted under the approval of the research Tissue Banks (ethics reference 10/H1008/72 and 08/H0304/56+5).

Small sections of airways were dissected from the surrounding tissue and the resulting explants were smeared across the bottom of one well of a 6-well plate. Cells were grown out from explants cultured in DMEM supplemented with 10% of FCS and 5% of PSF.

2.5 | HEK293 cell culture

GloResponse™ CRE-luc2P HEK293 cells (Promega, E8500) were grown in Dulbecco's Modified Eagles Medium with 4500 mg/L glucose, L-glutamine, and sodium bicarbonate, without sodium pyruvate (DMEM) with the addition of 10% FCS with 50 µg/ml hygromycin B.

2.6 | Recombinant cell line production

GloResponse™ CRE-luc2P HEK293 cells were transfected using Fugene® 6 (Promega) with a lentivirus plasmid containing full length GPR126 and the puromycin resistance gene at a 1.5:1 Fugene: DNA ratio using the protocol was provided by the manufacturer. Cells expressing GPR126 were selected by puromycin treatment. Plasmids were designed and purchased from VectorBuilder (Chicago, USA).

2.7 | Luciferase assays

Transfected cells were seeded into 96-well plate 24 hours prior to stimulation and treated with the stachel peptide (1 mM) or other agonists for 4 hours. Bright-Glo buffer and Bright-Glo substrate (Promega) were mixed and 100 µl of the solution was added to each well of a 96-well plate to terminate the assay. Plates were incubated at room temperature for at least 2 minutes before luminescence was measured on a Flexstation 3 microplate reader (Molecular Devices) for 0.5 seconds/well.

2.8 | cAMP assays

cAMP responses were measured as previously described.[36] In brief, HBEC and HASM cultures were seeded into 24-well plate 24 hours prior to treatments. Cell cultures were loaded with ^{3}H adenine for 2 hours. Cells were washed with serum-free media prior to stimulation. Experiments were stopped and cells were lysed by adding concentrated HCl. ^{14}C-cAMP was added to each well to allow for normalization across the columns. The contents of each well were then transferred to Dowex columns and three milliliters of H_2O was added to wash each column. Dowex columns were placed on top of

alumina columns. Six milliliters of H_2O was added to dowex columns and allowed to drip through both sets of columns. Dowex columns were removed and the alumina columns were placed over scintillation vials. Five milliliters of 0.1 M of imidazole was applied and allowed to drip through the columns into the scintillation vials. Ten milliliters of scintillation fluid was added to each vial and vials were counted on a Packard Scintillation counter using a $^{3}H/^{14}C$ dual-count program for 5 minutes per vial. cAMP accumulation was calculated by normalizing ^{3}H counts per well to ^{14}C counts. Each condition was performed in three replicate wells.

2.9 | Library preparation for RNA-sequencing

Library preparation and RNA-sequencing were carried out by Oxford Genomics Centre. RNA was quantified using RiboGreen (Invitrogen, Glasgow, UK) on the FLUOstar OPTIMA plate reader (BMG Labtech, Aylesbury, UK) and the size profile and integrity analyzed on the 4200 TapeStation (Agilent). RNA was normalized to 100 ng prior to library preparation. Polyadenylated transcript enrichment and strand-specific library preparation were completed using NEBNext Ultra II mRNA kit (NEB, Hitchin, UK) following the manufacturer's instructions. Libraries were amplified on a Tetrad (Bio-Rad, London, UK) using in-house unique dual-indexing primers. Individual libraries were normalized using Qubit, and the size profile was analyzed on the 4200 TapeStation. Individual libraries were normalized and pooled together accordingly. The pooled library was diluted to ~10 nM for storage. The 10 nM library was denatured and further diluted prior to loading on the sequencer.

2.10 | RNA-sequencing

Paired end (75 bp) sequencing was performed using a HiSeq4000 platform and HiSeq 3000/4000 PE Cluster Kit and 150 cycle SBS Kit (Illumina, Cambridge, UK), generating a raw read count of ~30 million reads per sample.

2.11 | Analysis of RNA-sequencing data

Processing of the RNA-sequencing data was performed using a Unix operating system. Adaptor sequence and quality trimming were performed using Scythe (https://github.com/vsbuffalo/scythe) and Sickle (https://github.com/najoshi/sickle), respectively. Alignment of RNA-Seq reads to genome build GRCh37 was carried out using Tophat package.[37] Analysis of trimmed RNA-sequencing files was performed using the Cufflinks package[37] as we have done previously.[38] Cuffdiff and Cuffnorm were used to determine differential (5% FDR) and gene expression was normalized to library size, respectively. Gene set enrichment analysis was performed using the GSEA software from the Broad Institute and the Molecular Signatures Database (MSigDB).[39,40] Volcano plots and heatmaps were produced in RStudio using ggplot2[41] and pheatmap,[42] respectively.

3 | RESULTS

3.1 | Variants on chromosome 6 associated with lung function alter GPR126 amino acid sequence and affect GPR126 expression levels

To identify causal variants underlying the two association signals with FEV_1/FVC ratio, we sought to identify SNPs which could be potentially causative. This included identifying SNPs which have regulatory effects such as expression quantitative trait loci (eQTLs) and non-synonymous variants using GTEx Portal V8 Release (https://www.gtexportal.org/home/)[43] and Open Target Genetics (https://genetics.opentargets.org/). We also used LDlink and HaploReg V4.1 to identify additional variants that were in linkage disequilibrium (LD) with the two sentinel variants ($r^2 > 0.1$).

Signal 1 (rs17280293) results in missense variant Ser123Gly. Using LDlink, we identified 64 SNPs in LD with signal 1 ($r^2 > 0.1$) including missense variant rs11155242 ((Lys230Gln), $r^2 = 0.1442$, D' = 1). Neither SNP is an eQTL for *GPR126* expression in lung tissue in the GTEx database (V8 release). However rs17280293 is an eQTL for *GPR126* expression in blood (eQTLGen database)[44] with the G allele (higher lung function) associated with reduced *GPR126* expression (beta: −0.205, pval:7.1e-16). In addition, rs11155242 (C, correlated with rs17280293 G) is an eQTL for *GPR126* in a number of tissues including blood, macrophage, monocytes, and T-Cells.[45] SIFT[46] and PolyPhen-2[47] were used to assess potential pathogenicity of these two coding region variants. Both tools predicted rs17280293 to be damaging to protein function potentially via the insertion of a smaller amino acid and loss of structure and rs11155242 to be benign/tolerated.

Signal 2 had 262 SNPs in LD ($r^2 > 0.1$) and is in linkage equilibrium with rs17280293 (r^2: 0.0836) suggesting independence from signal 1. Within this LD block there are two SNPs associated with scoliosis rs41289839 ($r^2 = 0.1746$) and rs6570507 ($r^2 = 0.9006$) with rs7753012. The signal 2 sentinel SNP (rs7753012) is an eQTL for *GPR126* expression in the esophagus with the G allele (higher lung function) associated with lower expression of GPR126 (NES: -0.15, pval: 0.000031). Moreover, the two scoliosis SNPs are also eQTLs for *GPR126* in other tissues including blood, cultured fibroblasts, and skeletal muscle.[43]

3.2 | GPR126 is expressed in human lung tissue and structural airway cells

To determine the expression profile of GPR126 in human structural airway cells, we performed RNA-sequencing on RNA extracted from HASM cells and HBECs. HBECs were from healthy donors purchased from Lonza (Wokingham, UK) and HASM cells were grown from lung tissue donors. Normalized expression values are shown as the number of fragments per kilobase of transcript per million mapped reads (FPKM). *GPR126* is expressed in both cell types, with higher expression levels observed in HBEC (n = 9 donors, mean = 17.5 FPKM, min = 6.3, and max = 27.1) compared with HASM (n = 5 donors, mean = 5.7 FPKM, min = 0.3, and max = 19.2) (Figure 1A).

In order to assess if *GPR126* expression in human lung tissue varies in disease states such as COPD, we utilized RNA-seq datasets available on the Gene Expression Omnibus (GEO). We searched the database with the following search terms; Lung tissue, airway smooth muscle, bronchial epithelial, COPD, and RNA-seq. We identified two datasets which allow comparison of gene expression in lung tissue/cell types between COPD and control.

GSE57148 contains a dataset comparing lung tissue from patients with normal spirometry vs tissue from COPD patients.[48] *GPR126* expression is expressed in human lung tissue and at significantly higher levels in COPD patients vs controls (COPD FPKM median 10.5, control FPKM median 9.1, and $P = .0164$) (Figure 1B). GSE124180 contains RNA-seq data from large airway epithelium, alveolar macrophage, and peripheral blood samples from COPD cases and controls.[49] Differential expression of GPR126 was not observed in large airway epithelium, alveolar macrophages, or peripheral blood between controls and COPD patients, although sample numbers were low (Figure 1C-E).

3.3 | Adhesion GPCR expression in structural airway cells

To contextualize the expression levels of GPR126, we analyzed RNA-seq data in HASM and HBECs for the wider

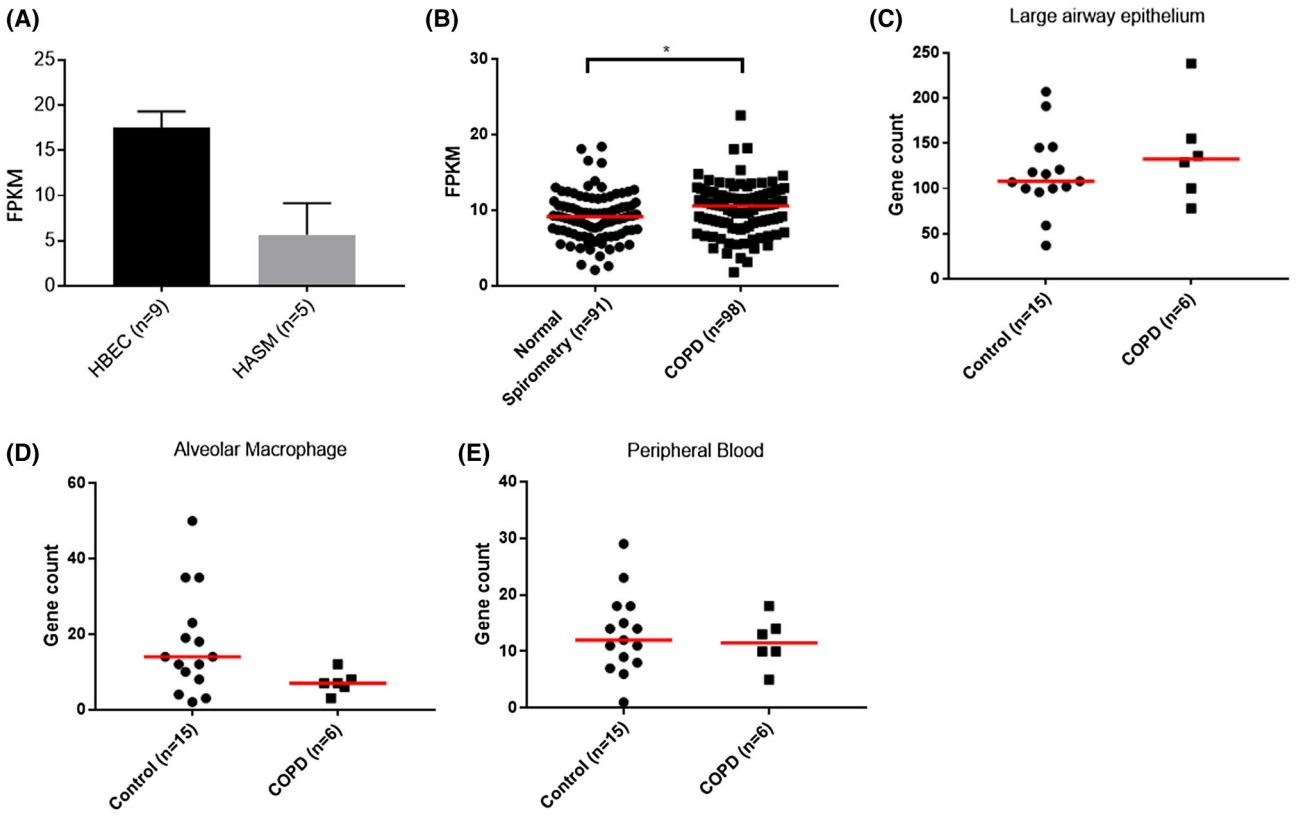

FIGURE 1 Average FPKM values for all donors is shown for HBECs (n = 9) and HASMs (n = 5) (A). RNA-seq data from whole lung tissue was downloaded from GEO (GSE57148) and GPR126 expression was compared in RNA extracted from healthy lung tissue and lung tissue from COPD patients (B). FPKM values from control (mean = 9.1, min = 2.1, and max=18.4) and COPD patients (mean = 10.1, min = 1.7, and max=22.5) were compared using an unpaired *t* test. Data were normally distributed as determined by a Shapiro-Wilk normality test. GPR126 expression in COPD vs controls was compared in GSE124180 in different cell types (C-E). No significant differences in expression between COPD and control were observed

family of aGPCRs as well as the expression levels of a well-studied airway GPCR for comparison, the β-2 adrenergic receptor (*ADRB2*) (Table 1). Seventeen of the 33 aGPCRs are expressed in at least one cell type and *GPR126* is expressed in both HASM and HBEC at higher levels than *ADRB2*.

3.4 | GPR126 signals via cAMP-mediated pathways in structural airway cells

In order to assess GPR126 signaling activity and effects of the Ser123Gly variant to potential ligands, we produced a recombinant cell system using the GloResponse™ CRE-luc2P HEK293 Cell Line (Promega) to overexpress human GPR126. We created cells lines expressing the Ser123 and Gly123 variants of the receptor. Cells were treated with collagen type IV (3 μg/ml) and laminin-211 (200 ng/μl) for 4 hours; however neither agonist induced signaling.[23,28] Cells were then treated with the activating peptide stachel (1 mM) for 5 hours[17] and we observed a dose-dependent increase in luciferase activity in cells expressing both variants but no increase in signal in empty vector or no vector controls (Figure 2A). However, we did not identify any genotype-specific effects. We also measured cAMP accumulation in these same cells using column chromatography, showing increased levels of cAMP after 1 mM stachel treatment at 1 and 4 hours (Figure 2B).

We then tested whether stachel could activate GPR126 signaling in primary cultured human airway structural cells. HASM cells and HBECs were treated with stachel peptide (1 mM) for 1 hour with pre-incubation with IBMX (10 uM). Accumulation of cAMP was measured using column chromatography. In HASM cells we observed a mean fold increase in cAMP of 21.5 ± 3.4 ($P = .0079$) and in HBECs a more modest but still significant response (2.1 ± 0.5 mean fold increase ($P = .0278$)) (Figure 2C-D).

TABLE 1 Median and range expression (in FPKM) of the adhesion GPCR family of receptors in HASM cells (n = 5) and HBECs (n = 9)

Adhesion GPCR	Average FPKM in HBEC (n = 9)	Average FPKM in HASM cells (n = 5)
ADGRA2 (GPR124)	0.1 (0-1.6)	24.3 (15.2-38.9)
ADGRA3 (GPR125)	18.6 (13.6-29)	11.4 (9.1-13.2)
ADGRB2 (BAI2)	1.2 (0.4-2.4)	5.9 (2.9-12.2)
ADGRC1 (CELSR1)	45.5 (31.3-55.9)	0.9 (0.2-1.8)
ADGRC2 (CELSR2)	17.6 (9.4-37.2)	1 (0.23-2.2)
ADGRC3 (CELSR3)	19 (0.6-25.5)	0.8 (0.3-1.2)
ADGRD1 (GPR133)	0 (0.008-0.012)	9.6 (0.2-34.4)
ADGRE5 (CD97)	10 (1.5-13.3)	24 (6-32.2)
ADGRF1 (GPR110)	10.6 (2.6-29.9)	0 (0-0)
ADGRF2 (GPR111)	17.9 (13-24.9)	0.1 (0-0.3)
ADGRF4 (GPR115)	17.9 (13-24.9)	0.1 (0-0.3)
ADGRG1 (GPR56)	107.3 (67.7-149.2)	3.2 (0.3-6.2)
ADGRG2 (GPR64)	0.1 (0.04-0.35)	0.4 (0.2-0.6)
ADGRG6 (GPR126)	17.5 (6.3-27.1)	5.7 (0.2-19.2)
ADGRL1 (LPHN1, CIRL-1, and CL1)	1.9 (0.7-2.8)	2 (1.3-2.3)
ADGRL2 (LPHN2, CIRL-2, and CL2)	15.3 (10.2-26)	14.4 (8.5-22.9)
ADGRL4 (ELTD1 and ETL)	0.2 (0-0.7)	6 (3.8-11)
ADRB2	14.9 (8.5-32.8)	4 (0.1-8.5)

Note: Only aGPCRs with FPKM >1 in either HASM cells or HBECs are included in the table except GPR64.

3.5 | GPR126 expression increases as cells become more confluent and after stachel stimulation

These data show that activation of cAMP-driven gene expression occurs after stimulation of GPR126 expressing cells with stachel peptide. Therefore, to gain insight into potential biological functions driven by changes in gene expression in HASM and identify downstream targets of GPR126 activation, we treated HASM cells with stachel (1 mM) for 4 and 24 hours and performed RNA-sequencing. Cuffnorm was used to generate normalized expression values (FPKM) for individual genes and isoforms in HASM cells (n = 4 independent experiments, one donor). *GPR126* is expressed at higher levels 24 hours after treatment and is significantly elevated after stachel treatment for 24 hours compared to basal and scrambled ($P = .0071$) (Figure 3). There was no significant difference in *GPR126* expression between the different conditions after 4 hours.

3.6 | GPR126 activation results in differential regulation of >300 genes

To assess the downstream genes and pathways and, therefore, potential biological implications of GPR126 activation, we used Cuffdiff to assess differentially regulated genes between HASM cells treated with stachel and those treated with a scrambled control peptide. GPR126 activation by stachel peptide in HASM cells resulted in 345 (135 upregulated and 210 downregulated) and 356 (109 upregulated and 247 downregulated) differentially expressed genes at 4 (Figure 4) and 24 hours (Figure 5), respectively, vs a scrambled control peptide. These data are based on 1% FDR and we only considered genes which had a baseline expression of FPKM >1. At 4 hours, top genes (defined by q value then fold change) included *FAM150A*, *KRTAP2-3*, *ARID5A*, *ATP8B1*,

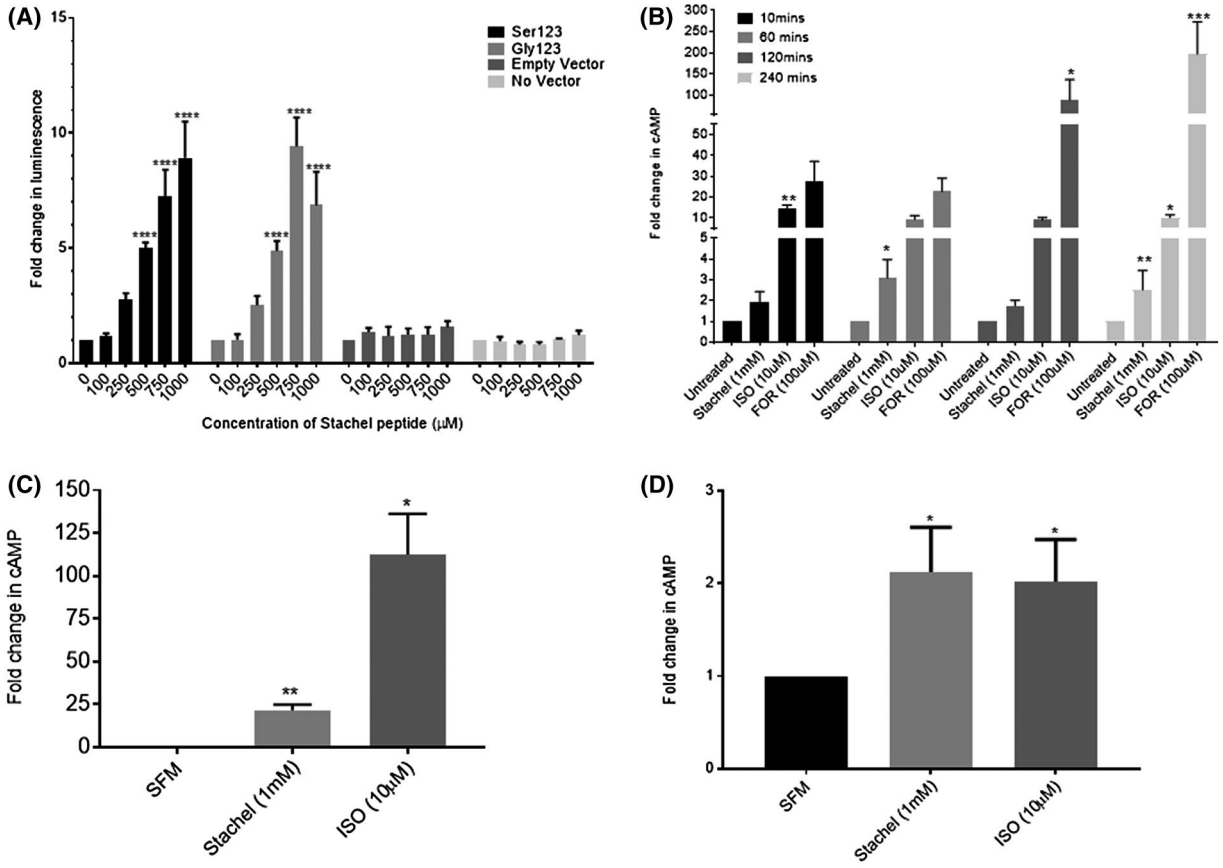

FIGURE 2 Luciferase response of HEK293 cells transfected with GPR126 to increasing concentrations (100-1000μM) of the stachel peptide after 5 hours of incubation (n = 5) (A). cAMP measurements in $GPR126^{Ser123}$ and $GPR126^{Gly123}$ HEK293 cells in response to stachel peptide, isoprenaline, and forskolin treatment for 10, 60, 120, and 240 minutes with pre-treatment with IBMX (B). cAMP accumulation in HASM cells (C) and HBECs (D) pre-treated with IBMX and then, treated with Stachel (1 mM) or isoprenaline (10 μM) for 1 hour (n = 5). Data shown are mean ± SEM. SFM, serum free media

ANKRD1, *HDAC9*, *KRTAP1-5*, *CTGF*, *NLRP10*, and *KLHL38* (all downregulated) and *SYT12*, *ZBTB7C*, *HEATR6*, *IFI27*, *SLC16A9*, *TMEM100*, *ZNF813*, *ADAM8*, *PDE3A*, and *RASD2* (all upregulated). At 24 hours top downregulated genes were *RP11-87N24.3*, *snoU13*, *SERPINE1*, *TM4SF20*, *OXTR*, *LAD1*, *TNNT2*, *ANO1*, *MAP3K7CL*, and *ACTG2* and upregulated genes were *ZBTB7C*, *TMEM100*, *CACNA1G*, *PTPRN*, *LRRN3*, *PLP1*, *HTRA3*, *YPEL4*, *RNF112*, and *SLITRK6*. The full list of differentially expressed genes can be found in Supplementary Table 3 (4 hours) and Table 4 (24 hours).

3.7 | Genes implicated in airway diseases are regulated by GPR126 activation

After identifying genes which were differentially regulated at the two time points, we compared the genes differentially expressed at 4 hours to those at 24 hours. We found that ~20% of genes were differentially regulated by GPR126 activation with the same direction of effect with 40 upregulated and 74 downregulated (Figure 6A). To focus our analysis, we then looked at the genes which were differentially expressed using an arbitrary cut off of a ≥2 fold change in either direction at both time points (Figure 6B). There were 26 genes that met this criteria, these include genes with previously reported roles in airway disease such as IL33 (upregulated), CTGF (downregulated), and SERPINE1 (downregulated).[50-52]

3.8 | Pathway analyses suggests GPR126 may have a role in cell proliferation

Gene Set Enrichment Analysis (GSEA) was used from the Broad Institute to identify gene sets/biological pathways effected by GPR126 activation.[40] There were nine gene sets that were enriched (1% FDR) by GPR126 activation in the hallmark gene sets. No gene sets were enriched at 4 hours using the hallmark gene set. The differentially regulated gene sets at 24 hours are involved in cell cycle regulation and cell proliferation (Table 2). These processes are known to be

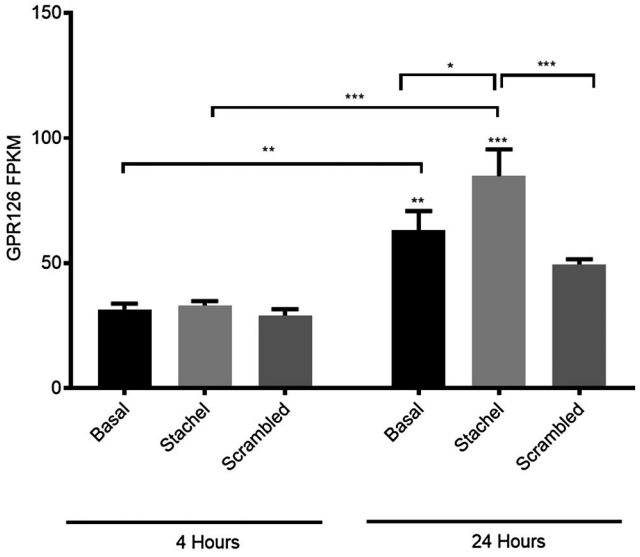

FIGURE 3 GPR126 mRNA expression increases over time in cultured HASM which is augmented by stachel peptide stimulation of cells. GPR126 mRNA expression in basal HASM cells, cells treated with stachel (1 mM) or scrambled-treated cells at 4 and 24 hours. FPKM values for each condition were compared between the two time points using a two-way ANOVA with Sidak's multiple comparisons test. In addition, FPKM values were compared within each time point for each condition using a two-way ANOVA with Tukey's multiple comparisons test. Data shown are mean ± SEM from four experiments

regulated by aGPCRs in other cell types. We also analyzed the list of differentiated genes (1% FDR) through The Database for Annotation, Visualization, and Integrated Discovery (DAVID).[53] The most significant results grouped differentially expressed genes into Mitosis ($P = 2.23E-06$), cell division ($P = 1.54E-03$), and cell cycle ($P = 9.11E-03$).

4 | DISCUSSION

In this study, we hypothesized that genetic variants that affect GPR126 expression or function may contribute to processes that lead to airway disease. We aimed to identify potential causal variants driving the GWAS association signals observed for FEV_1/FVC and explore the potential role of GPR126 in human airway structural cells. Signal 1 has a coding region sentinel SNP resulting in Ser123Gly, a variant predicted to be damaging to protein function, but in recombinant cell experiments we were unable to detect any altered signaling as a consequence of this polymorphism. The signal 2 top variant however is an eQTL in a range of tissue types where it has been studied, suggesting that altered GPR126 expression could be driving at least some of the genetic associations seen. We identified GPR126 expression in the lung and in HASMs and HBECs and identified that GPR126 could have a role in airway remodeling via transcriptomic analysis.

From the analysis of the LD structure around the sentinel SNPs, the most compelling SNP for further analysis was the Ser123Gly variant (signal 1), predicted to be damaging to protein function. Based on the genetics from the Shrine et al, 2019 GWAS, the Ser123 allele (common) is protective against lung function decline.

However, we were unable to detect a functional effect of the Ser123Gly variant in recombinant cell models. There are several potential explanations for this. First, stachel binds C-terminal to the Ser123Gly position and, therefore, any potential effects of this amino acid change on ligand binding may be bypassed. We were unable to test any differential effects of the reported ligands collagen type IV and laminin 211 as these did not activate receptor signaling in our system. We cannot exclude that the recombinant expression system (higher than endogenous) altered the state of GPR126 and responsiveness to ligand. Second, we overexpressed the alpha 2 variant of the receptor, which lacks exon 6 of the full-length protein and this may, therefore, be a limitation. It has recently been shown that transcripts lacking exon 6 exist in a closed conformation and signal less readily than GPR126 transcripts with exon 6 present.[18] These factors may explain why signaling activity was not observed when cells were treated with collagen type IV or laminin 211. However, we saw robust effects on signaling in both cell lines and also in primary cultured HASM cells following activation with the stachel peptide suggesting any genotype-specific effects should have been found with the transcript we expressed.

Our eQTL analyses suggest that alleles associated with higher lung function are associated with reduced GPR126 mRNA expression levels. Similarly, we identified elevated GPR126 mRNA levels in lung tissue from COPD patients vs normal spirometry controls. Therefore, we hypothesis that increased expression/activity of GPR126 may be damaging in the lung. We chose to study this in airway smooth muscle, given that eQTL signals were observed in fibroblast and smooth muscle containing tissues.

Given the potential for altered gene expression to be driving effects of GPR126 signaling, we therefore, used RNA-seq to identify the potential roles of GPR126 in HASMs by activating the receptor with the activating peptide stachel. GPR126 activation by stachel peptide resulted in 345 and 356 differentially expressed genes at 4 and 24 hours, respectively. There were distinct transcriptome profiles at the two time points with a ~20% overlap of common differentially regulated genes. Therefore, while the two time points may identify early and late response genes, there is increased confidence that the genes differentially regulated at both time points are driven by real effects of GPR126 activation. The genes differentially regulated following the activation of GPR126 are predominantly in pathways controlling mitosis and cell division.

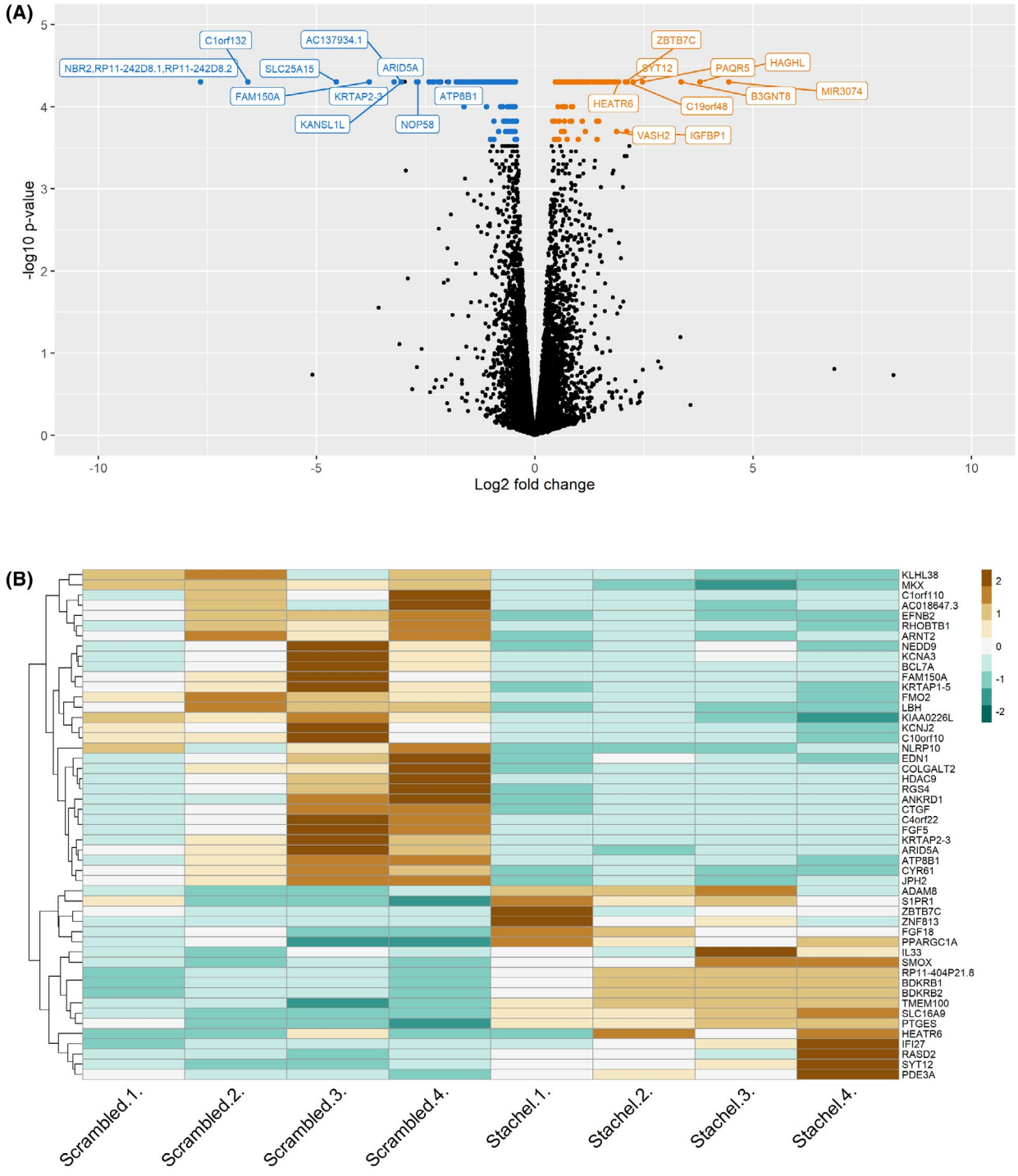

FIGURE 4 Volcano plot shows differentially expressed (1% FDR, FKPM >1) genes after stachel treatment vs scrambled control after 4 hours. Genes which are labeled are the top 10 genes ranked first by q value then by fold change. Colored dots represent genes which reach 1% FDR. Heatmaps show gene expression across individual replicate experiments. Genes shown are the top 50 ranked first by q value then by fold change. Genes which were not differentially regulated in three out of four replicates were removed. Brown represents upregulation and green represents downregulation

We also found that *GPR126* mRNA expression in HASMs generally increases over time in culture. One potential explanation for the increase in *GPR126* expression at 24 hours may be that the cells were more confluent and, therefore, there are more cell-cell and cell-matrix interactions. As the cells proliferate, more matrix is deposited and an increase in matrix would be expected to include matrix ligands for GPR126. aGPCRs are known to modulate a number of cellular functions including cell migration, adhesion, polarity, and guidance via these adhesion interactions.[54] Moreover, it

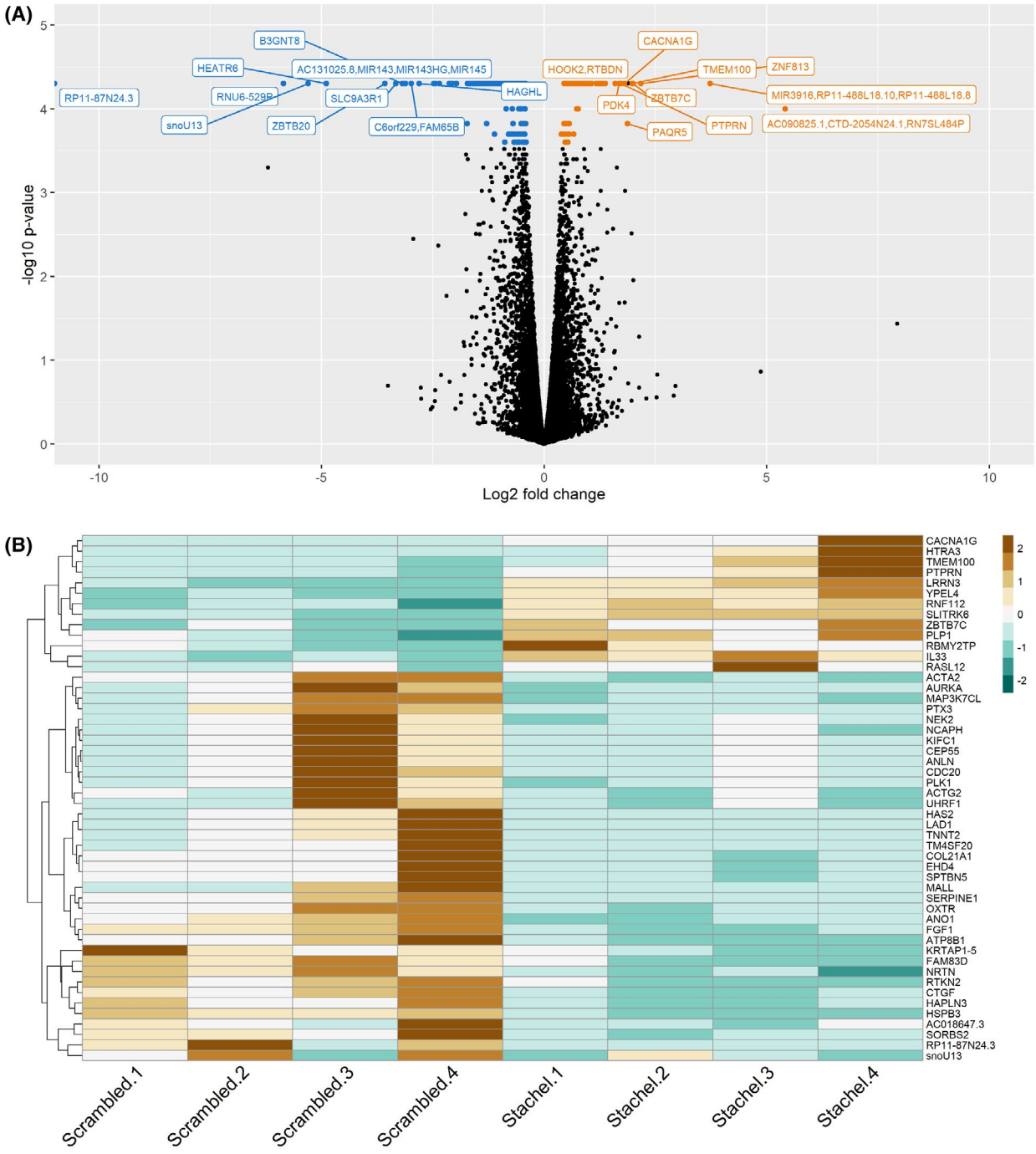

FIGURE 5 Volcano plot shows differentially expressed (1% FDR, FKPM >1) genes after stachel treatment vs scrambled control after 24 hours. Genes which are labeled are the top 10 genes ranked first by q value then by fold change. Colored dots represent genes which reach 1% FDR. Heatmaps show gene expression across individual replicate experiments. Genes shown are the top 50 ranked first by q value then by fold change. Genes which were not differentially regulated in three out of four replicates were removed. Brown represents upregulation and green represents downregulation

is also known that GPR126 is vital for normal tissue development via interactions with the ECM.[23,28] Therefore, GPR126 may be upregulated to facilitate these functions when there is increased cell-cell and cell-matrix contact. GPR126 activity also increased after stachel treatment providing evidence for a positive feedback loop. This may also explain increased *GPR126* expression in lung tissue from COPD patients. We did not directly test the relationship between GPR126 expression and cAMP signaling.

Differentially regulated genes after stachel activation include IL33, CTGF, and SERPINE1, all of which have known roles in airway disease and present possible mechanisms for

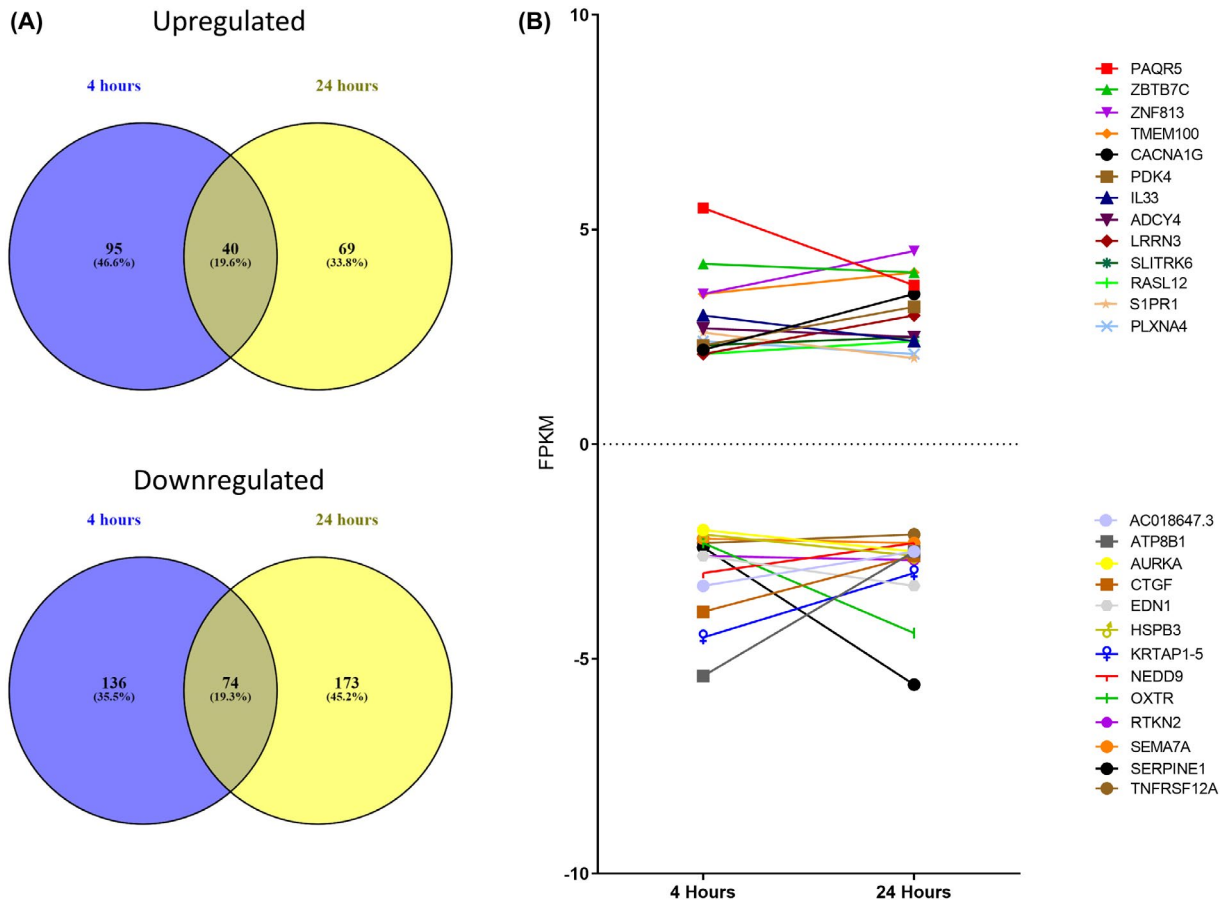

FIGURE 6 Differentially expressed genes at both time points (A). Fold change in FPKM at both time points. Genes shown are those which are differentially expressed at both time points with a fold change ≥ 2 and GPR126 (B)

GPR126 involvement in airway disease. Chronic inflammation of the airways is a key feature of many diseases causing airflow obstruction and airway smooth muscle secretes a variety of chemokines and cytokines that can perpetuate airway inflammation.[55] For example, IL33 (upregulated by GPR126 activation) is a well characterized cytokine that plays an important role in several chronic inflammatory diseases by promoting inflammatory cytokine production.[56] Serum levels of IL-33 and its receptor ST2 are elevated in patients with COPD compared to control subjects and peripheral blood lymphocytes from COPD patients release more IL33 in response to stimulus than healthy controls.[52] As GPR126 activation upregulated IL33 expression, reduced GPR126 expression in individuals carrying the protective alleles could potentially result in less IL33 being produced although this requires further investigation.

Airway remodeling results from a wide range of mechanisms involving smooth muscle cell hyperplasia, increased activation of fibroblasts and myofibroblasts, increased deposition of the ECM, and aberrant inflammatory responses. Airway smooth muscle undergoes alterations in health and disease characterized by cell proliferation, hypertrophy, and migration, and the expression of chemokines and cytokines is important in regulating airway inflammation.[55] Furthermore, smooth muscle mass is altered in COPD due to hypertrophy and hyperplasia.[55] We observed increased GPR126 expression in more confluent smooth muscle cells and, therefore, perhaps increased smooth muscle mass or ECM deposition in COPD is responsible for increased GPR126 expression observed in lung tissue from COPD patients.

CTGF is a gene downregulated by GPR126 activation which has roles in inflammation and tissue remodeling. This ECM protein recruits fibroblasts to wound sites, along with other inflammatory mediators such as TGF-β and IL-8/CXCL8. *CTGF* has a known role in pulmonary fibrosis and airway remodeling and has been shown to modulate a number of signaling pathways involved in cell adhesion and migration, angiogenesis, myofibroblast activation, and extracellular matrix deposition, which together can result in tissue remodeling and fibrosis.[51] These processes are also in keeping with what is known about adhesion GPCR biology.[10] Elevated CTGF expression contributes to expression of ECM proteins, cell migration, and the myofibroblastic phenotype in tissue repair.[57] In mouse lung tissue, CTGF expression and promoter activity are elevated after bleomycin challenge.[58] CTGF exerts profibrotic effects and

TABLE 2 Nine gene sets are downregulated by GPR126 activation in the hallmark gene sets

Gene sets	Pathways	Size	ES	NES	q value (FDR)	Leading edge	Time point
Hallmark	E2F targets	199	−0.71	−2.04	0	tags = 66%, list = 14%, and signal = 76%	24 hours
Hallmark	MYC targets	199	−0.7	−1.97	0	tags = 67%, list = 19%, and signal = 83%	24 hours
Hallmark	G2M checkpoint	199	−0.68	−1.93	0	tags = 60%, list = 12%, and signal = 68%	24 hours
Hallmark	MTORC1 signaling	199	−0.62	−1.74	0.001	tags = 63%, list = 18%, and signal = 76%	24 hours
Hallmark	MYC targets v2	58	−0.68	−1.65	0.0033	tags = 62%, list = 18%, and signal=75%	24 hours

Note: Size = number of genes in the gene set after filtering out those not in the expression dataset. ES = enrichment score for the gene set. This is the degree to which the gene set is overrepresented at the top or bottom of the ranked list of genes in the expression dataset. NES = normalized enrichment score. q value = false discovery rate—the estimated probability that the NES represents a false positive. Leading edge subset = subset of members that contribute the most to the ES. Tags = the percentage of genes contributing to the ES. List = percentage of genes in the ranked gene list before the peak in the running ES. This gives an indication of where in the list the ES is attained. Signal = the ES strength that combines the two previous statistics.

contributes to lung fibrosis via transcriptional regulation of COL1A2.[58] Altered CTGF expression might seem unlikely to mediate the effects of GPR126 variants as expression was downregulated following GPR126 activation, although increased remodeling would be expected to lead to a reduced FVC and hence downregulation of CTGF could be working through this route.

SERPINE1 (PAI-1) (also downregulated by GPR126 activation) has been shown to be upregulated in emphysema lung and increased expression of PAI-1 suppresses fibrinolysis leading to pathological fibrin deposition and tissue damage.[50,59] Moreover, PAI-1 knockout mice display an emphysema-like phenotype, possibly due to an imbalance in protease-antiproteases activity in the lung—a known factor in emphysema development.[60] Elevated levels of PAI-1 are observed in the sputum of COPD patients and these levels were more elevated in more severe COPD cases.[61,62] PAI-1 plays a critical role in fibrosis development in a number of tissues including in the lung[63] and is produced by smooth muscle cells.[59] As with CTGF, the direction of effect following GPR126 activation initially seems inconsistent with altered SERPINE1 levels mediating effects of GPR126 activation but again this could be working through increased FVC rather than altered FEV_1.

In addition to potential roles in inflammation and remodeling, GPR126 activation resulted in the differential regulation of genes within pathways involved in proliferation and cell cycle regulation. It has also been recently shown that GPR126 knockdown results in an increased proliferation of pulmonary artery smooth muscle cells where increased expression of GPR126 was associated with decreased proliferation.[64] These results are consistent with our suggestion that GPR126 plays a role in control of cell proliferation in the lungs.

There are limitations to our study. First, we were unable to detect GPR126 protein expression due to technical challenges and, therefore, we were unable to confirm cell surface expression of GPR126 in our recombinant cell system and in the primary cells. Moreover, as we were unable to detect signaling using identified GPR126 ligands we chose to use the GPR126 stachel peptide, which has been shown to cross-activate other receptors within and across aGPCR families. For example, peptides derived from GPR64 and GPR126 do cross-activate their respective receptors.[65] However, the peptide from GPR126 shows higher potency and efficacy on its originating receptor. To address this, we assessed GPR64 expression levels in HASM cells and HBECs prior to experimentation. Expression of GPR64 was at the lowest level of detection with FPKM <1 (Table 1). These data provided some confidence the signal was GPR126 derived, however we cannot completely exclude the possibility that GPR64 may make a minor contribution to signaling.

Collectively, these differentially expressed genes and pathways highlight a potential novel role for GPR126 in regulating the connected processes of airway remodeling and airway inflammation—both key processes in the pathophysiology of COPD. The genetic analyses suggest that GPR126 increased expression/activity may be damaging and we hypothesize that this could result in dysregulation of pathways involved in smooth muscle cell proliferation which may, therefore, contribute to airway disease.

ACKNOWLEDGMENTS

IS received the following grants; Hermes Fellowship (University of Nottingham, 2016-2017), British Lung Foundation (Grant PPRG15-5). IPH holds a NIHR Senior Investigator award. This work was partially supported by an MRC programme grant (G1000861). Lung tissue samples were obtained and research conducted under the approval of the Nottingham Health Science Biobank and Papworth Hospital Research Tissue Bank.

CONFLICT OF INTEREST

The authors state that there are no conflict of interest in connection with this article.

AUTHOR CONTRIBUTIONS

I Sayers and I P Hall conceived and designed the study. R Hall designed and completed the experiments and analyzed the data. J O'Loughlin, C K Billington, and D Thakker completed the experiments. I Sayers, I P Hall, and R J Hall wrote the paper with contributions from all authors.

ORCID

Robert J. Hall https://orcid.org/0000-0001-9114-7144

REFERENCES

1. Soriano JB, Abajobir AA, Abate KH, et al. Global, regional, and national deaths, prevalence, disability-adjusted life years, and years lived with disability for chronic obstructive pulmonary disease and asthma, 1990–2015: a systematic analysis for the Global Burden of Disease Study 2015. *Lancet Respir Med*. 2017;5:691-706.
2. Langenhan T, Aust G, Hamann J. Sticky signaling–adhesion class G protein-coupled receptors take the stage. *Sci Signal*. 2013;6:re3.
3. Klimentidis YC, Vazquez AI, de Los Campos G, Allison DB, Dransfield MT, Thannickal VJ. Heritability of pulmonary function estimated from pedigree and whole-genome markers. *Front Genet*. 2013;4:174.
4. Shrine N, Guyatt AL, Erzurumluoglu AM, et al. New genetic signals for lung function highlight pathways and chronic obstructive pulmonary disease associations across multiple ancestries. *Nat Genet*. 2019;51:481-493.
5. Hobbs BD, de Jong K, Lamontagne M, et al. Genetic loci associated with chronic obstructive pulmonary disease overlap with loci for lung function and pulmonary fibrosis. *Nat Genet*. 2017;49:426-432.
6. Soler Artigas M, Wain LV, Miller S, et al. Sixteen new lung function signals identified through 1000 Genomes Project reference panel imputation. *Nat Commun*. 2015;6:8658.
7. Hancock DB, Eijgelsheim M, Wilk JB, et al. Meta-analyses of genome-wide association studies identify multiple loci associated with pulmonary function. *Nat Genet*. 2010;42:45-52.
8. Terzikhan N, Sun F, Verhamme FM, et al. Heritability and genome-wide association study of diffusing capacity of the lung. *Eur Respir J*. 2018;52:1800647.
9. Bjarnadottir TK, Fredriksson R, Schioth HB. The adhesion GPCRs: a unique family of G protein-coupled receptors with important roles in both central and peripheral tissues. *CMLS*. 2007;64:2104-2119.
10. Yona S, Lin HH, Siu WO, Gordon S, Stacey M. Adhesion-GPCRs: emerging roles for novel receptors. *Trends Biochem Sci*. 2008;33:491-500.
11. Krasnoperov V, Lu Y, Buryanovsky L, Neubert TA, Ichtchenko K, Petrenko AG. Post-translational proteolytic processing of the calcium-independent receptor of alpha-latrotoxin (CIRL), a natural chimera of the cell adhesion protein and the G protein-coupled receptor. Role of the G protein-coupled receptor proteolysis site (GPS) motif. *J Biol Chem*. 2002;277:46518-46526.
12. Arac D, Boucard AA, Bolliger MF, et al. A novel evolutionarily conserved domain of cell-adhesion GPCRs mediates autoproteolysis. *EMBO J*. 2012;31:1364-1378.
13. Chang GW, Stacey M, Kwakkenbos MJ, Hamann J, Gordon S, Lin HH. Proteolytic cleavage of the EMR2 receptor requires both the extracellular stalk and the GPS motif. *FEBS Lett*. 2003;547:145-150.
14. Paavola KJ, Stephenson JR, Ritter SL, Alter SP, Hall RA. The N terminus of the adhesion G protein-coupled receptor GPR56 controls receptor signaling activity. *J Biol Chem*. 2011;286:28914-28921.
15. Paavola KJ, Hall RA. Adhesion G protein-coupled receptors: signaling, pharmacology, and mechanisms of activation. *Mol Pharmacol*. 2012;82:777-783.
16. Musa G, Cazorla-Vázquez S, van Amerongen MJ, et al. Gpr126 (Adgrg6) is expressed in cell types known to be exposed to mechanical stimuli. *Ann N Y Acad Sci*. 2019;1456:96-108.
17. Liebscher I, Schon J, Petersen SC, et al. A tethered agonist within the ectodomain activates the adhesion G protein-coupled receptors GPR126 and GPR133. *Cell Rep*. 2014;9:2018-2026.
18. Xu E, Shao W, Jiang H, Lin T, Gao R, Zhou X. A genetic variant in GPR126 causing a decreased inclusion of Exon 6 is associated with cartilage development in adolescent idiopathic scoliosis population. *Biomed Res Int*. 2019;2019:4678969.
19. Mogha A, Benesh AE, Patra C, et al. Gpr126 functions in Schwann cells to control differentiation and myelination via G-protein activation. *J Neurosci*. 2013;33:17976-17985.
20. Cui H, Wang Y, Huang H, et al. GPR126 protein regulates developmental and pathological angiogenesis through modulation of VEGFR2 receptor signaling. *J Biol Chem*. 2014;289:34871-34885.
21. Geng FS, Abbas L, Baxendale S, et al. Semicircular canal morphogenesis in the zebrafish inner ear requires the function of gpr126 (lauscher), an adhesion class G protein-coupled receptor gene. *Development (Cambridge, England)*. 2013;140:4362-4374.
22. Monk KR, Oshima K, Jors S, Heller S, Talbot WS. Gpr126 is essential for peripheral nerve development and myelination in mammals. *Development (Cambridge, England)*. 2011;138:2673-2680.
23. Petersen SC, Luo R, Liebscher I, et al. The adhesion GPCR GPR126 has distinct, domain-dependent functions in Schwann cell development mediated by interaction with laminin-211. *Neuron*. 2015;85:755-769.
24. Monk KR, Naylor SG, Glenn TD, et al. A G protein-coupled receptor is essential for Schwann cells to initiate myelination. *Science (New York, N.Y.)*. 2009;325:1402-1405.
25. Glenn TD, Talbot WS. Analysis of Gpr126 function defines distinct mechanisms controlling the initiation and maturation of myelin. *Development (Cambridge, England)*. 2013;140:3167-3175.
26. Waller-Evans H, Promel S, Langenhan T, et al. The orphan adhesion-GPCR GPR126 is required for embryonic development in the mouse. *PLoS One*. 2010;5:e14047.
27. Patra C, van Amerongen MJ, Ghosh S, et al. Organ-specific function of adhesion G protein-coupled receptor GPR126 is domain-dependent. *Proc Natl Acad Sci USA*. 2013;110:16898-16903.
28. Paavola KJ, Sidik H, Zuchero JB, Eckart M, Talbot WS. Type IV collagen is an activating ligand for the adhesion G protein-coupled receptor GPR126. *Sci Signal*. 2014;7:ra76.
29. Leon K, Cunningham RL, Riback JA, et al. Structural basis for adhesion G protein-coupled receptor Gpr126 function. *Nat Commun*. 2020;11:194.
30. Kou I, Takahashi Y, Johnson TA, et al. Genetic variants in GPR126 are associated with adolescent idiopathic scoliosis. *Nat Genet*. 2013;45:676-679.
31. Xu JF, Yang GH, Pan XH, et al. Association of GPR126 gene polymorphism with adolescent idiopathic scoliosis in Chinese populations. *Genomics*. 2015;105:101-107.
32. Qin X, Xu L, Xia C, et al. Genetic variant of GPR126 gene is functionally associated with adolescent idiopathic scoliosis in Chinese population. *Spine*. 2017;42:E1098-E1103.

33. Kou I, Watanabe K, Takahashi Y, et al. A multi-ethnic meta-analysis confirms the association of rs6570507 with adolescent idiopathic scoliosis. *Sci Rep*. 2018;8:11575.
34. Miller S, Melen E, Merid SK, Hall IP, Sayers I. Genes associated with polymorphic variants predicting lung function are differentially expressed during human lung development. *Respir Res*. 2016;17:95.
35. Rayner RE, Makena P, Prasad GL, Cormet-Boyaka E. Optimization of normal human bronchial epithelial (NHBE) cell 3D Cultures For In Vitro Lung Model Studies. *Sci Rep*. 2019;9:500.
36. Billington CK, Pascual RM, Hawkins ML, Penn RB, Hall IP. Interleukin-1beta and rhinovirus sensitize adenylyl cyclase in human airway smooth-muscle cells. *Am J Respir Cell Mol Biol*. 2001;24:633-639.
37. Trapnell C, Roberts A, Goff L, et al. Differential gene and transcript expression analysis of RNA-seq experiments with TopHat and Cufflinks. *Nat Protoc*. 2012;7:562-578.
38. Kheirallah AK, de Moor CH, Faiz A, Sayers I, Hall IP. Lung function associated gene Integrator Complex subunit 12 regulates protein synthesis pathways. *BMC Genom*. 2017;18:248.
39. Liberzon A, Birger C, Thorvaldsdottir H, Ghandi M, Mesirov JP, Tamayo P. The molecular signatures database (MSigDB) hallmark gene set collection. *Cell Syst*. 2015;1:417-425.
40. Subramanian A, Tamayo P, Mootha VK, et al. Gene set enrichment analysis: a knowledge-based approach for interpreting genome-wide expression profiles. *Proc Natl Acad Sci USA*. 2005;102:15545-15550.
41. Wickham H. *ggplot2: Elegant Graphics for Data Analysis*. Springer International Publishing; 2016.
42. Kolde R.pheatmap: Pretty Heatmaps. 2019.
43. The GC. The genotype-tissue expression (GTEx) project. *Nat Genet*. 2013;45:580-585.
44. Võsa U, Claringbould A, Westra H-J, et al. Unraveling the polygenic architecture of complex traits using blood eQTL metaanalysis. *bioRxiv*. 2018;447367.
45. Carvalho-Silva D, Pierleoni A, Pignatelli M, et al. Open targets platform: new developments and updates two years on. *Nucleic Acids Res*. 2018;47:D1056-D1065.
46. Kumar P, Henikoff S, Ng PC. Predicting the effects of coding non-synonymous variants on protein function using the SIFT algorithm. *Nat Protoc*. 2009;4:1073-1081.
47. Adzhubei IA, Schmidt S, Peshkin L, et al. A method and server for predicting damaging missense mutations. *Nat Meth*. 2010;7:248-249.
48. Kim WJ, Lim JH, Lee JS, Lee SD, Kim JH, Oh YM. Comprehensive analysis of transcriptome sequencing data in the lung tissues of COPD subjects. *Int J Genom*. 2015;2015:206937.
49. Morrow JD, Chase RP, Parker MM, et al. RNA-sequencing across three matched tissues reveals shared and tissue-specific gene expression and pathway signatures of COPD. *Respir Res*. 2019;20:65.
50. Savarimuthu Francis SM, Davidson MR, Tan ME, et al. MicroRNA-34c is associated with emphysema severity and modulates SERPINE1 expression. *BMC Genom*. 2014;15:88.
51. Lipson KE, Wong C, Teng Y, Spong S. CTGF is a central mediator of tissue remodeling and fibrosis and its inhibition can reverse the process of fibrosis. *Fibrogenesis Tissue Repair*. 2012;5:S24.
52. Xia J, Zhao J, Shang J, et al. Increased IL-33 expression in chronic obstructive pulmonary disease. *Am J Physiol-Lung Cell Mol Physiol*. 2015;308:L619-L627.
53. da Huang W, Sherman BT, Lempicki RA. Systematic and integrative analysis of large gene lists using DAVID bioinformatics resources. *Nat Protoc*. 2009;4:44-57.
54. Hamann J, Aust G, Arac D, et al. International union of basic and clinical pharmacology. XCIV. Adhesion G protein-coupled receptors. *Pharmacol Rev*. 2015;67:338-367.
55. Panettieri RA Jr, Kotlikoff MI, Gerthoffer WT, et al. Airway smooth muscle in bronchial tone, inflammation, and remodeling: basic knowledge to clinical relevance. *Am J Respir Crit Care Med*. 2008;177:248-252.
56. Shang J, Zhao J, Wu X, Xu Y, Xie J, Zhao J. Interleukin-33 promotes inflammatory cytokine production in chronic airway inflammation. *Biochem Cell Biol*. 2015;93:359-366.
57. Lin CH, Shih CH, Tseng CC, et al. CXCL12 induces connective tissue growth factor expression in human lung fibroblasts through the Rac1/ERK, JNK, and AP-1 pathways. *PLoS One*. 2014;9:e104746.
58. Ponticos M, Holmes AM, Shi-wen X, et al. Pivotal role of connective tissue growth factor in lung fibrosis: MAPK-dependent transcriptional activation of type I collagen. *Arthritis Rheum*. 2009;60:2142-2155.
59. Cesari M, Pahor M, Incalzi RA. Plasminogen activator inhibitor-1 (PAI-1): a key factor linking fibrinolysis and age-related subclinical and clinical conditions. *Cardiovasc Ther*. 2010;28:e72-e91.
60. Hu H, Zhao Y, Xiao Y, Zhang R, Song H. Disruption of plasminogen activator inhibitor-1 gene enhances spontaneous enlargement of mouse airspace with increasing age. *Tohoku J Exp Med*. 2010;222:291-296.
61. To M, Takagi D, Akashi K, et al. Sputum plasminogen activator inhibitor-1 elevation by oxidative stress-dependent nuclear factor-kappaB activation in COPD. *Chest*. 2013;144:515-521.
62. Jiang Y, Xiao W, Zhang Y, Xing Y. Urokinase-type plasminogen activator system and human cationic antimicrobial protein 18 in serum and induced sputum of patients with chronic obstructive pulmonary disease. *Respirology (Carlton, Vic)*. 2010;15:939-946.
63. Ghosh AK, Vaughan DE. PAI-1 in tissue fibrosis. *J Cell Physiol*. 2012;227:493-507.
64. Gorr MW, Sriram K, Muthusamy A, Insel PA. Transcriptomic analysis of pulmonary artery smooth muscle cells identifies new potential therapeutic targets for idiopathic pulmonary arterial hypertension. *Br J Pharmacol*. 2020;177:3505-3518.
65. Demberg LM, Winkler J, Wilde C, et al. Activation of adhesion G protein-coupled receptors: agonist specificity of stachel sequence-derived peptides. *J Biol Chem*. 2017;292:4383-4394.

SUPPORTING INFORMATION

Additional Supporting Information may be found online in the Supporting Information section.

How to cite this article: Hall RJ, O'Loughlin J, Billington CK, Thakker D, Hall IP, Sayers I. Functional genomics of GPR126 in airway smooth muscle and bronchial epithelial cells. *The FASEB Journal*. 2021;35:e21300. https://doi.org/10.1096/fj.202002073R